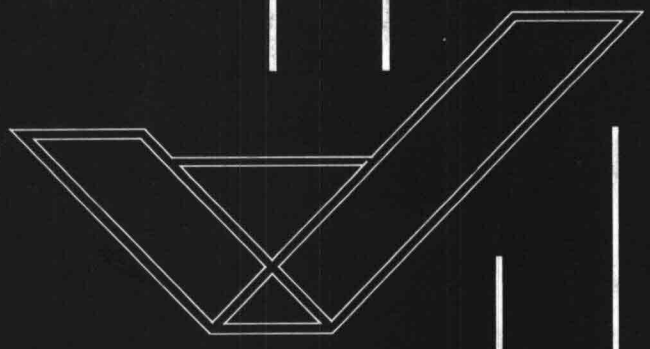

SIMULATION OF FLOW IN RIVERS AND TIDAL CHANNELS WITH AN IMPLICIT FINITE DIFFERENCE METHOD OF THE ADI-TYPE

Joh.G.S. Pennekamp and R. Booij

Report no. 3 - 83

Laboratory of Fluid Mechanics
Department of Civil Engineering
Delft University of Technology

SIMULATION OF FLOW IN RIVERS AND TIDAL CHANNELS WITH AN IMPLICIT FINITE DIFFERENCE METHOD OF THE ADI-TYPE

Joh.G.S. Pennekamp and R. Booij

Report No. 3 - 83

Laboratory of Fluid Mechanics
Department of Civil Engineering
Delft University of Technology

Contents

List of Figures

1. Introduction

In order to make predictions for the morphology of an alluvial bottom a thorough knowledge of the flow pattern is needed. In tidal channels, without a nett discharge over the tidal period, the main flow effects on the morphology will, on an average, remain relatively small because of the tidal variation. Therefore second order flow phenomena become important. In particular the secondary flow is important, because it gives rise to bottom slopes transverse to the main flow.

This research, which is financially supported by the directorate of the Deltadienst of Rijkswaterstaat, concerns the determination of the secondary flow in tidal channels like estuaries as the Eastern Scheldt based on a known depth averaged velocity field. The depth averaged velocities must be computed with a high accuracy in order to make a reasonable determination of the secondary flow. For the computation of depth averaged velocities usually an implicit finite difference method of the ADI-type is used.

In these methods the depth averaged equations of motion, together with the depth averaged continuity equation, together called the shallow water equations, are solved by means of an Alternating Direction Implicit computation using a spatial staggered grid.

A simplification of the effective stress term in the shallow water equations is made to economize the computation.

Although the velocity parameters andwater level parameter are treated implicitly, the convective and diffusion terms are represented explicitly in the difference equations, which can give rise to instability of the numerical computation. The computation is executed with an imposed diffusion coefficient in order to suppress this instability.

In this report an investigation is done concerning the diffusion coefficient and its influence on the velocity distribution in a steady or quasi-steady flow in rivers and estuaries.

Estimates of the physical lateral viscosity for the same flows are made and their influence on the velocity distribution is discussed.

In the overall research of which this report covers just a part, the accuracy of the derived calculation of the secondary flow will be verified with measurements of the flow in the curved flume of the Delft Hydraulic Laboratory (de Vriend, 1978).

At the Laboratory of Fluid Mechanics a flume with a 180-degrees bend is available in which also measurements are planned for the use of verification of the secondary flow model.

It is found that the velocity distribution in these flume models is severely influenced by the imposed diffusion coefficient corresponding with a reasonable time step, so no accurate velocity field can be computed using the implicit finite difference method in the current form without requiring expensive computations

Some attention has been paid to the rectangular representation of the curvilinear boundaries.

2. Mathematical description

2.1. The shallow-water equations

In flow-problems in coastal waters, estuaries and rivers it is usually fairly justified to assume a hydrostatic pressure distribution along the vertical, i.e. the vertical accelerations are negligibly small.

Integration over depth of the Reynolds' equations for turbulent flow in three dimensions and assuming a hydrostatic pressure distribution yields the differential equations for two dimensional horizontal flow, the shallow water equations (Flokstra, 1976), which read:

$$\frac{\partial u}{\partial t} + u\frac{\partial u}{\partial x} + v\frac{\partial u}{\partial y} + g\frac{\partial \zeta}{\partial x} + \frac{1}{\rho h}(\tau_{bx} - \tau_{wx}) - \Omega v + $$

$$- \frac{1}{\rho h}\frac{\partial (hT_{xx})}{\partial x} - \frac{1}{\rho h}\frac{\partial (hT_{xy})}{\partial y} = 0 \qquad (1)$$

$$\frac{\partial v}{\partial t} + u\frac{\partial v}{\partial x} + v\frac{\partial v}{\partial y} + g\frac{\partial \zeta}{\partial y} + \frac{1}{\rho h}(\tau_{by} - \tau_{wy}) + \Omega u + $$

$$- \frac{1}{\rho h}\frac{\partial (hT_{xy})}{\partial x} - \frac{1}{\rho h}\frac{\partial (hT_{yy})}{\partial y} = 0 \qquad (2)$$

$$\frac{\partial \zeta}{\partial t} + \frac{\partial (hu)}{\partial x} + \frac{\partial (hv)}{\partial y} = 0 \qquad (3)$$

In these equations the following notation is used (see also definition sketch, fig. 1):

x,y	horizontal coordinates;
u,v	depth-averaged velocity-component in x-,y-direction;
ζ	waterlevel above reference level;
g	acceleration due to gravity;
h	waterdepth;
ρ	mass density;
τ_{bx}, τ_{by}	components of bottom shear stress;
τ_{wx}, τ_{wy}	components of surface shear stress;
Ω	Coriolis parameter: $2\omega \sin\phi$, where ϕ is the geographic latitude and ω is the angular velocity of the rotation of the earth;
T_{xx}, T_{xy}, T_{yy}	effective stresses in vertical planes.

Usually the bottom shear stresses are assumed to act opposite to the direction of the mean velocity vector and to vary with the mean velocity squared:

$$\tau_{bx} = \frac{\rho g}{C^2} u \sqrt{u^2+v^2} \tag{4}$$

$$\tau_{by} = \frac{\rho g}{C^2} v \sqrt{u^2+v^2} \tag{5}$$

in which C is the Chézy coefficient.

The complete expressions for the effective stresses (Flokstra, 1981) are:

$$T_{xx} = \frac{1}{h} \int_{z_b}^{z_b+h} \{2\rho\nu \frac{\partial \hat{u}}{\partial x} - \rho\overline{u'^2} - \rho(\hat{u}-u)^2\}dz \tag{6}$$

$$T_{xy} = \frac{1}{h} \int_{z_b}^{z_b+h} \{\rho\nu (\frac{\partial \hat{u}}{\partial y} + \frac{\partial \hat{v}}{\partial x}) - \rho\overline{u'v'} - \rho(\hat{u}-u)(\hat{v}-v)\}dz \tag{7}$$

$$T_{yy} = \frac{1}{h} \int_{z_b}^{z_b+h} \{2\rho\nu \frac{\partial \hat{v}}{\partial y} - \rho\overline{v'^2} - \rho(\hat{v}-v)^2\}dz \tag{8}$$

where: ν is the kinematic coefficient of viscosity;

$\hat{u}$, $\hat{v}$ are the depth-dependent values of the velocities.

Each effective stress expression consists of three components with different physical meaning. The first part is the vertical mean viscous stress (at sufficiently high values of the Reynolds number this contribution may be neglected). The second contribution concerns the turbulent stress acting in vertical planes.
The third contribution represents the momentum flux due to the non-uniform vertical distribution of the velocity. This third contribution, its character and its effect on the flow are discussed further in (2.2).

In current numerical models the shallow water equations are modified. The effective stress term is substituted bij a single diffusion term with a constant diffusion coefficient. (Vreugdenhil - Wijbenga, 1982, Booij - de Boer, 1981). With this modification and the bottom stress assumption the shallow water equations (4,5) can be rewritten into

$$\frac{\partial u}{\partial t} + u\frac{\partial u}{\partial x} + v\frac{\partial u}{\partial y} + g\frac{\partial \zeta}{\partial x} + \frac{g}{C^2}\frac{u\sqrt{u^2+v^2}}{h} + W_x - \Omega v$$

$$- \frac{\partial}{\partial x}(\varepsilon_p \frac{\partial u}{\partial x}) - \frac{\partial}{\partial y}(\varepsilon_p \frac{\partial u}{\partial y}) = 0 \qquad (9)$$

$$\frac{\partial v}{\partial t} + u\frac{\partial v}{\partial x} + v\frac{\partial v}{\partial y} + g\frac{\partial \zeta}{\partial y} + \frac{g}{C^2}\frac{v\sqrt{u^2+v^2}}{h} + W_y + \Omega u$$

$$- \frac{\partial}{\partial x}(\varepsilon_p \frac{\partial v}{\partial x}) + \frac{\partial}{\partial y}(\varepsilon_p \frac{\partial v}{\partial y}) = 0 \qquad (10)$$

$$\frac{\partial \zeta}{\partial t} + \frac{\partial (hu)}{\partial x} + \frac{\partial (hv)}{\partial y} = 0 \qquad (11)$$

Usually the equations are further simplified by supposing ε_p to be a constant throughout the flow.

These shallow water equations result in a system of equations which can be solved in a numerical way. Most of the numerical models for the integration of these equations are based on the implicit finite difference scheme as proposed by Leendertse (1967).

2.2. The momentum flux due to the non-uniform velocity distribution

The effective stresses (see equations 6, 7, 8) are combinations of viscous stresses, Reynolds stresses, and momentum fluxes due to the non-uniform distributions of the velocities over the depth. For the flow problems considered in this report, the viscous stresses can be neglected in comparison with the Reynolds stresses. The momentum fluxes due to the velocity distribution can be large compared to the Reynolds stresses, but some comments on their part in the equations of motion (1,2) are appropriate.

If the velocity profiles in the x- and in the y-direction are similar, which in general is approximately the case in shallow water flow, then these momentum fluxes can be considered small corrections on the momentum fluxes due to convection.

$$\frac{1}{h}\int_{z_b}^{z_b+h} \rho(\hat{u}-u)^2 dz = \rho\alpha u^2 \tag{12}$$

$$\frac{1}{h}\int_{z_b}^{z_b+h} \rho(\hat{u}-u)(\hat{v}-v) dz = \rho\alpha uv \tag{13}$$

$$\frac{1}{h}\int_{z_b}^{z_b+h} \rho(\hat{v}-v)^2 dz = \rho\alpha v^2 \tag{14}$$

with in case of a logarithmic vertical distribution of the velocity

$$\alpha = \frac{g}{\kappa^2 C^2} \tag{15}$$

where κ is Von Karman's constant and α is a constant depending on the shape of the velocity profile.

In the equations of motions (1,2) the stresses give rise to the terms

$$\frac{\partial}{\partial x}\alpha u^2 + \frac{\partial}{\partial y}\alpha uv = \alpha(2u\frac{\partial u}{\partial x} + u\frac{\partial v}{\partial y} + v\frac{\partial u}{\partial y}) \simeq \alpha(u\frac{\partial u}{\partial x} + v\frac{\partial u}{\partial y}) \tag{16}$$

and

$$\frac{\partial}{\partial x}\alpha uv + \frac{\partial}{\partial y}\alpha v^2 \simeq \alpha(u\frac{\partial v}{\partial x} + v\frac{\partial v}{\partial y}) \tag{17}$$

These terms mean small corrections on the convection terms in the equations of motion.

$$u\frac{\partial u}{\partial x} + v\frac{\partial u}{\partial y} \qquad \text{and} \qquad u\frac{\partial v}{\partial x} + v\frac{\partial v}{\partial y} \tag{18}$$

For $C = 50\ m^{\frac{1}{2}}/s$ expression (15) gives $\alpha \simeq 1/40$, so the corrections on the convection terms are small and generally negligible.

In river or channel bends and suddenly expanding rivers and channels, where circulations develop, the velocity profiles in the x-direction and the y-direction can differ as a result of secondary flow. An analogous difference between the velocity profiles can appear in estuaries as a result of secondary flow due to the Coriolis force (Booij and Kalkwijk, 1982). The difference is best recognized when one coordinate axis is chosen in the main flow direction. An outward transport of the main flow in river bends (Kalkwijk and de Vriend, 1980) is caused by the momentum fluxes due to these non-uniform velocity distributions (In case of secondary flow due to the Coriolis effect this term causes a transport of the main flow to the right). This effect is not reproduced when these momentum fluxes are accounted for by diffusion terms.

It can be concluded that the part of the momentum fluxes due to the non-uniform vertical velocity profiles can generally be neglected when secondary flow is not important. When secondary flow is important, then these momentum fluxes can not be neglected, but they can certainly not be replaced by diffusion terms.

Neglect of the share of the momentum fluxes due to non-uniform velocity distribution in the equations of motion (1, 2) and use of the eddy viscosity concept yields shallow water equations of the form:

$$\frac{\partial u}{\partial t} + u\frac{\partial u}{\partial x} + v\frac{\partial u}{\partial y} + g\frac{\partial \zeta}{\partial x} + \frac{g}{C^2}\frac{u\sqrt{u^2+v^2}}{h} + W_x - \Omega v - \frac{\partial}{\partial x}\left(\nu_t \frac{\partial u}{\partial x}\right) -$$

$$- \frac{\partial}{\partial y}\left(\nu_t \frac{\partial u}{\partial y}\right) = 0 \qquad (19)$$

$$\frac{\partial v}{\partial t} + u\frac{\partial v}{\partial x} + v\frac{\partial v}{\partial y} + g\frac{\partial \zeta}{\partial y} + \frac{g}{C^2}\frac{v\sqrt{u^2+v^2}}{h} + W_y + \Omega u - \frac{\partial}{\partial x}\left(\nu_t \frac{\partial v}{\partial x}\right) -$$

$$- \frac{\partial}{\partial y}\left(\nu_t \frac{\partial v}{\partial y}\right) = 0 \qquad (20)$$

These equations are equal to equations (9, 10). Only the lateral eddy viscosity ν_t replaces the diffusion coefficient ε_p. In equations (19, 20) the current bottom stresses assumption (equations 4, 5) is used.

3. Numerical method

3.1. Computational description

The modified shallow water differential equations (9, 10, 11) can be solved by an implicit finite difference method (Leendertse, 1967; Booij - de Boer, 1981). This method is of an Alternating - Direction - Implicit (ADI)-type. In an alternating way each half timestep the equations in the x- and y-direction respectively are solved by means of an implicit computation. The non-linear terms are represented in such a way that a tridiagonal system of linear equations arises along each row or column of grid points. Each system of equations can independently be solved together with the corresponding boundary conditions. The convective terms and diffusion terms are treated explicitly. The convective terms are represented by central differences using values from the older time level and therefore can give rise to instability in the computation.

Vreugdenhil and Wijbenga(1982) note that to a certain extent the accuracy of this numerical method can be judged by its truncation error. They state that part of the truncation error has the form of a numerical diffusion term with a negative value:

$$- \beta U^2 \Delta t \left(\frac{\partial^2 u}{\partial s^2} , \frac{\partial^2 v}{\partial s^2} \right) \qquad (21)$$

in which U is the magnitude of the velocity, s is the local flow direction, β is a constant and Δt is the numerical time increment used in the computation. This effect (21) works only during the unsteady state, in the steady state it is cancelled by other terms in the truncation error.

3.2. Stability criteria

From the numerical diffusion coefficient a stability criterion can be derived. Noting that the local diffusion coefficient should at least be positive in order to get a stable computation, the criterion becomes:

$$\varepsilon - \beta U^2 \Delta t > 0 \qquad \text{or} \qquad \Delta t < \frac{\varepsilon}{\beta U^2} \qquad (22)$$

where ε denotes the imposed diffusion coefficient used in the numerical computation. In the steady state no imposed diffusion is compensated by the negative numerical diffusion term arising from the truncation error, because the effect of the negative numerical diffusion is cancelled by other terms with in the truncation error. Nevertheless the amount of imposed diffusion is needed to prevent small disturbances from growing. In the steady state or quasi-steady state e.g. tidal channel flow, the total imposed diffusion will influence the results of the computation.

In the publication of Vreugdenhil and Wijbenga(1982), the coefficient β is set equal to $\frac{1}{4}$. According to Vreugdenhil this value is not exact; it may vary with the used computational model. The exact value of β is hard to determine. Nevertheless when the shallow water equations are solved with use of an implicit finite difference scheme based upon Leendertse (1967) the part of the truncation error that has the form of a diffusion term will have a diffusion coefficient of the form $\beta U^2 \Delta t$.

With the inequality (22) an instability region in the $\Delta t - \varepsilon$ plane is defined. For the diffusion equation, computed with an explicit method, it can be shown that the stability criterion

$$\frac{2\varepsilon \Delta t}{\Delta x^2} < 1 \qquad (23)$$

applies (Kuipers and Vreugdenhil, 1973). Usually the diffusion terms are treated explicitely in the implicit finite difference methods under discussion. Therefore the stability criterion (23) also holds for these computations.

The two stability criteria (22, 23) outline a region in the ε-Δt plane in which the computation will be stable for a given spatial grid distance Δx. Thus the stability region for a certain Δx can be plotted as shown below.

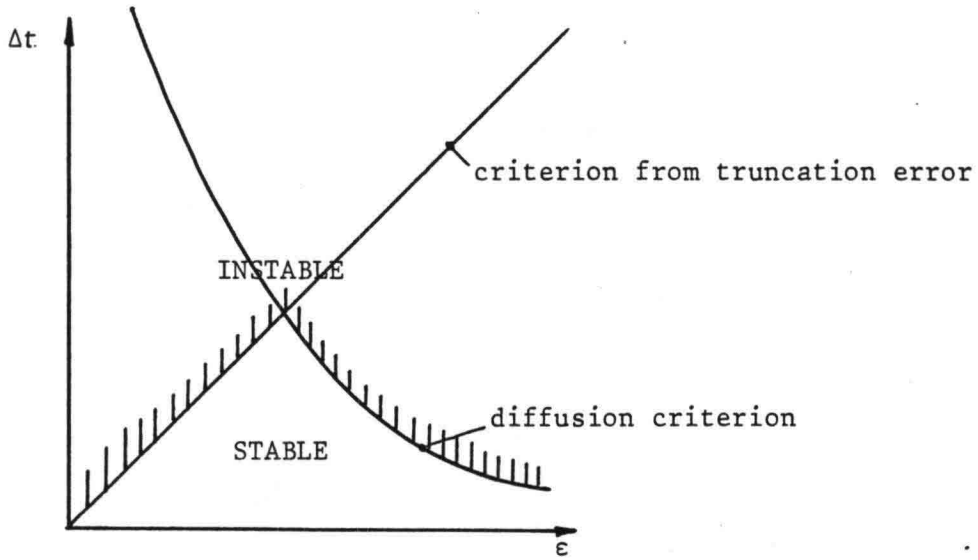

This figure shows that for a given spatial grid distance (Δx) the time increment (Δt) reaches a maximum at a certain diffusioncoefficient. In view of stability this can be considered as an optimum. For instance, take for a tidal channel with a width of 1000 m and a maximum velocity of 1.5 m/s, a grid size of 50 or 75 m, then the timestep cannot exceed 47 and 70 s respectively (see fig. 2). These time steps can only result in a stabile computation if the imposed diffusion coefficient is fixed on 26.5 m^2/s and 39.5 m^2/s respectively.

3.3. Instability in different flow configurations

When the computation with an implicit finite difference method of the ADI-type for a flow through a flume results in an instable computation for a certain time step, it can be shown that every other flow with Froude-scaled dimensions similar to the flow will also show an instable computation if a time step scaled according to the time scale is used. Froude-scaling denotes that all the dimensions and flow parameters are scaled in such a way that the second flow has the same Froude number as the first flow.

The reason that instability will occur more easily in a certain configuration than in another one is, that the magnitudes of the convective terms in the basic equations (9, 10) are different.

4. Lateral viscosity

In chapter 3 two stability criteria for numerical computations of shallow water flows with implicit finite difference methods of the ADI-type were introduced. One of the criteria, expression (22), requires a lateral diffusion coefficient that is proportional to the time step used and to the square of the flow velocity. Generally a constant diffusion coefficient is chosen that is sufficiently large to obtain stability over the entire flow field.

The choice of the lateral diffusion coefficient can, however, severely influence the calculated velocity field. To examine the influence of the imposed lateral diffusion coefficient, it has to be compared to the lateral eddy viscosity ν_t in equations (19) and (20), when this latter mainly determines the velocities. When the flow is mainly controlled by the bottom friction, then the influence of the lateral diffusion coefficient on the velocity field has to be compared to the influence of this bottom friction.

4.1. Estimation of the lateral eddy viscosity

The lateral eddy viscosity ν_t can be estimated using the Reynolds analogy between turbulent momentum transport and turbulent mass transport. For wide straight channels the lateral diffusion coefficient for contaminants mentioned by Fischer et al. (1979) yields

$$\nu_t = 0.15\, u_* h \tag{24}$$

with u_* the shear stress velocity, defined by

$$u_* = \left(\frac{\tau_b}{\rho}\right)^{\frac{1}{2}} \tag{25}$$

in which τ_b is the bottom shear stress.

For rivers Fischer et al. (1979) mention a somewhat larger value ($\simeq 0.6\, u_* h$) for the diffusion coefficient for contaminants. The increase is caused by the considerable change in the vertical concentration profiles due to convection of the contaminant by the secondary flow in river bends. The vertical profiles of the longitudinal velocity are hardly influenced by the secondary flow, so the value of the eddy viscosity in straight channels (equation 24) seems to apply also for curved channels and rivers.

The eddy viscosity can be expressed in the depth-averaged velocity, using the expression

$$u_* = \frac{\sqrt{g}}{C} (u^2+v^2)^{\frac{1}{2}} \tag{26}$$

This gives for C = 50 $m^{\frac{1}{2}}/s$

$$\nu_t \simeq 0.01\ h(u^2+v^2)^{\frac{1}{2}} \tag{27}$$

To estimate the influence of the lateral eddy viscosity and the influence of the bed shear stress on the velocity field, a stationary flow, that is uniform in the longitudinal direction, in a straight channel with constant depth, is considered. The x-coordinate is chosen in the flow direction. In case of no surface shear stress and Coriolis effect equation (19) now becomes

$$g \frac{\partial \zeta}{\partial x} + \frac{\partial}{\partial y} (\nu_t \frac{\partial u}{\partial y}) + \frac{g\ u|u|}{C^2 h} = 0 \tag{28}$$

with a lateral eddy viscosity (see equation 27)

$$\nu_t \simeq 0.01\ hu \tag{29}$$

In shallow water flow the bed shear stress is generally predominant except near the sides of the channel. The region near the sides, where the influence of the lateral viscosity on the flow field is important, can be estimated in the following way. In this region the second term of equation (28) has to be at least of the same order of magnitude as the third term.

$$\frac{\partial}{\partial y} (\nu_t \frac{\partial u}{\partial y}) \gtrsim \frac{gu|u|}{C^2 h} \tag{30}$$

For C = 50 $m^{\frac{1}{2}}/s$ this amounts to

$$\frac{\partial^2 u}{\partial y^2} = \frac{1}{\nu_t} \frac{g\ u|u|}{C^2\ h} \simeq 2.5 \frac{u}{h^2} \tag{31}$$

, as can be seen by substituting equation (25), (26) and (29). So, the width of the region in which the lateral viscosity is important can be

estimated at about 1.6 h for C = 50 $m^{\frac{1}{2}}/s$. The lateral eddy viscosity will in reality decrease near the channel sides, yielding somewhat smaller side wall regions.

This characterization of the flow field compares well with measurements and computations mentioned by Rodi (1980), and with preliminary measurements in a straight section of a flume in the Laboratory of Fluid Mechanics of the Delft University of Technology (called henceforth the LFM flume). The width of the LFM flume is 60 cm. The water depth in the flume was 6 cm and the flow velocity was about 25 cm/s. The flow case mentioned by Rodi concerns measurements by Gonsovski (unpublished) and a computation with a depth-averaged version of the k-ε-model by Rastogi (unpublished) for a straight channel with a width to depth ratio of 30 (see figure 3).

In case of a depth variation in the direction normal to the flow, the influence of the lateral viscosity is consequently only perceptible near the place of variation. The considerations above apply also for non-stationary or weak non-uniform flows.

4.2. Influence of an imposed lateral diffusion coefficient

The lateral diffusion coefficient ε, imposed in computations of shallow water flow with an implicit finite difference method of the ADI-type, can have important consequences for the calculated velocity field, as is illustrated by the following example.

Vreugdenhil and Wijbenga (1982) computed the velocity field in the Meuse near Venlo, where the Meuse has a main channel with a width of 150 m, a depth of 9.5 m, C ≃ 60 $m^{\frac{1}{2}}/s$ and a mean velocity of about 1.5 m/s. The eddy viscosity can be computed using expressions (24) and (26)

$$\nu_t \simeq 0.11 \ m^2/s \qquad (32)$$

Vreugdenhil and Wijbenga used two different diffusion coefficients in their computation, viz. ε = 1 m^2/s and ε = 3 m^2/s, and compared the results to investigate the consequences of a difference in the value of the diffusion coefficient (see fig. 4).

The value of ν_t in expression (32) yields sidewall layers, in which the influence of the lateral eddy viscosity is important, with a width of about 2 h = 18 m (see page 14, with C ≃ 60 $m^{\frac{1}{2}}/s$). The values

of ε used by Vreugdenhil and Wijbenga (1982) yield much wider sidewall layers (using equation 31 with ε instead of ν_t), viz. about 70 m for $\varepsilon = 1$ m^2/s, and about 120 m for $\varepsilon = 3$ m^2/s. (Compare with figure 4).

The computations by Vreugdenhil and Wijbenga give even worse results then the analysis above suggests. The large friction caused by the large value of ε is compensated for by a decreased bottom friction (or higher Chézy coefficient). In this way the total resistance of the flow and the surface slope are correct, but the influence of the lateral viscosity is even increased.

Vreugdenhil and Wijbenga justify the large values of ε, by referring to an expression for the coefficient for the diffusion across a shear layer as given by Rodi (1980)

$$\varepsilon \simeq 0.01\ D\ \Delta u \tag{33}$$

in which D is the width of the shear layer and Δu is the velocity difference over the shear layer. Using for D half of the width of the Meuse and for Δu the mean velocity, ε becomes indeed 1.5 m^2/s. Vreugdenhil refers also to a paper of Lean and Weare (1979), who use a comparable expression. Lean and Weare, however, consider a channel, where the main flow expands on the downstream side of a breakwater. They use the expression only in a part of the mixing zone emanating from the breakwater tip. In the rest of the flow field they prefer expression (24), as the turbulence generated at the bed predominates except for the mixing region, where the turbulence generated by the horizontal velocity gradient is important.

For three flow situations the lateral eddy viscosity is given in table 1.

a) An example of the flow in a tidal channel. A width of 1000 m, an average depth of 20 m and a depth-averaged velocity of 1.5 m/s are used.
b) A flume in the Delft Hydraulics Laboratory with a width of 6 m, an average depth of 21 cm and an average velocity of 0.5 m/s (henceforth called the DHL flume).
c) The LFM flume (see page 15).

The lateral eddy viscosities in the three cases, using expression (29) for C = 50 $m^{\frac{1}{2}}/s$, are given in table 1.

	h	u	ν_t
Tidel Channel	20 m	1.5 m/s	0,3 m^2/s
DHL Flume	0.21 m	0.5 m/s	0.001 m^2/s
LFM Flume	0.06 m	0.25 m/s	0.00015 m^2/s

5. Boundary conditions

Two closed boundary conditions can be distinguished, the free-slip and the no-slip closed boundary condition. In both conditions 'closed' implies that there is no mass flux across the boundary:

$$u_n \Big|_b = 0 \tag{34}$$

where u_n is the local velocity in n-direction, perpendicular to the boundary.

In addition, for the free-slip closed boundary condition holds:

$$\varepsilon \frac{\partial u_s}{\partial n} \Big|_b = 0 \tag{35}$$

where u_s is the local velocity in s-direction, parallel to the boundary and ε is the lateral diffusion coefficient. Usually ε is fixed at a constant value everywhere throughout the flow. Equation (35) becomes (Vreugdenhil and Wijnbenga, 1982):

$$\frac{\partial u_s}{\partial n} \Big|_b = 0 \tag{36}$$

For the no-slip closed boundary condition holds:

$$u_s \Big|_b = 0 \tag{37}$$

When a boundary is represented in a numerical model by a rectangular grid the model boundaries are always parallel to the x-axis or y-axis of the grid, so n- and s-direction will always coincide with the orientation of either x- and y-direction or y- and x-direction.

The numerical treatment of these specific conditions may differ in the various models (Vreugdenhil 1973).

The no-slip condition will give rise to a boundary layer along the boundary. This phenomenon can dominate the velocity distribution along the width of the flume when a large lateral viscosity is used in order to maintain a stable computation. Consequently a larger fall of the energy head along the flow is needed because of the extra resistance of the boundary due to large lateral viscosity.

Some results of computations for the DHL-flume (see page 16) with the TIDES-package are plotted in fig. 5 . The TIDES-package (Booij - de Boer, 1981) has a computational scheme based on the implicit finite difference method, as discussed in 3.1, using an ADI-type computation. The computations were executed for the first straight part of the DHL-flume. At the upstream side of the flume a stationary velocity distribution along the width was imposed and at the downstream side of the flume a constant water level was maintained. Both these open boundary conditions, velocity distribution and water level, agreed with the corresponding measurements in the DHL-flume (de Vriend and Koch, 1978).

The theoretical velocity distribution in fig. 5 is based upon a calculation in which side wall friction and lateral viscosity are omitted and the velocity distribution is only determined by bottom friction. Neglect of the lateral viscosity in this case is justified according to the considerations discussed in 4.1. This theoretical distribution fits the measurements (de Vriend and Koch, 1978) very well as does the the slope of the water level.

Although the stability criteria allow any imposed diffusion coefficient with a sufficiently small time step to result in a stable computation, the required small time step has economical limitations. Smaller imposed diffusion coefficients will lead to more reliable results but to more expensive computations.

A reasonable time step is 2 seconds, which requires an imposed diffusion coefficient of 0.06 m^2/s in order to obtain a stable computation.

All the computations were executed until a steady flow was reached. Velocity distributions in case of free-slip condition and in case of no-slip condition at the closed boundaries are plotted in fig.5. In both cases the imposed diffusion coefficient was 0.06 m^2/s.

Figure 5 shows that the imposed diffusion coefficient influences the velocity distribution severely.

In the computed steady flow with no-slip closed boundary conditions the water level slope amounted to about four times the measured water level slope. In this case the imposed diffusion is responsible for a considerable energy dissipation as the no-slip conditions results in larger velocity gradients, especially near the side-walls, moreover the imposed diffusion coefficient has a constant value whereas the physical lateral viscosity decreases towards the side walls. The velocity distribution in the prototype shows large gradients in the regions with decreasing lateral viscosity. In case of free-slip closed boundary conditions only a slightly steeper water level slope, compared with the measured value, was found. Here the imposed diffusion flattens the velocity distribution, which provides higher velocities near the side walls of the flow. Near the side walls the water depth becomes smaller, the Chézy coefficient decreases, so the total bottom friction on the flow is larger that the measured value. Neither of the velocity distributions fits the measured values.

The velocity distribution of a computed steady flow with free-slip closed boundary conditions and with a lateral viscosity of 0.02 m^2/s is also represented in fig. 5. The maximum time step possible in this case, 0.5s, was used. This velocity distribution corresponds better with the measured distribution than the velocity distribution from the first computation using 0.06 m^2/s for the imposed diffusion coefficient (See 3.1).

To investigate the influence of the grid size on the velocity distribution, especially near the boundaries, computations were executed with half the grid distance of the former computations. Hardly any influence of the grid size was found. An example of these computations with an imposed diffusion coefficient of 0.06 m^2/s is represented in fig. 6 compared with the corresponding steady situation of the computation with the former grid size. The deviations of the velocity distribution near the boundaries are caused by the imposed free-slip closed boundary condition given bij Eq. 36. The mathematical description (36) is not equivalent with the physical free-slip condition, because the lateral eddy viscosity decreases rapidly near the boundary whereas the imposed diffusion coefficient is maintained at a constant value in the mathematical description.

6. Numerical representation of a curvilinear configuration by a rectangular grid

When in a numerical model for the simulation of a flow through a bend, the bend configuration is represented by a rectangular grid, it will be impossible to match the grid points everywhere with the physical wall boundary. The boundaries can only be approximated very roughly by a rectangular grid. This ill-matching of the numerical boundaries with the real boundaries gives rise to an additional flow resistance (Kuipers and Vreugdenhil, 1973). When a computation is set up for a stationary flow through a straight flume with a grid, correctly chosen, parallel to the flume axis, the results e.g. water level slope and velocity, will be the same as those of an analytical computation with corresponding Chézy coefficient values and lateral diffusion coefficient. When the computation for the flume is executed but now represented by a rectangular grid with another orientation with respect to the flume axis the value of the total resistance will increase with a considerable factor, so a steeper water level slope is needed to obtain the same discharge. The degree in which this numerical wall representation influences the main flow is dependent on the ratio of the width of the flow and the grid size. Smaller grid sizes in relation to a wider flow will result in smaller influence of the numerical wall representation.

Kuipers and Vreugdenhil (1973) have tried to reduce the influence of the wall representation by special treatments of the boundaries and modifications in the equations of motion. These treatments and modifications were artificial and although some final results, like friction and discharge, corresponded with the theoretical values the impact on other characteristics of the flow, for instance curvature of the streamlines, velocity distribution over the width, is not clear. No satisfactory treatment for the wall representation was found.

7. Economical aspects of the computation with an implicit finite difference method of the ADI-type

The stability criteria discussed in Chapter 3 impose strict limitations on the maximum time increment (Δt) that can be used in order to obtain a stable computation. In the next discussion some attention will be paid to the economical aspects of the use of an implicit finite difference method of the ADI-type, for the computation of tidal flows in estuaries. The specific implications of the introduction of a constant diffusion coefficient based on the consideration of stability are discussed in chapter 4.2.

As already pointed out in chapter 3 reasonable spatial grid-sizes Δx for tidal channel configurations are e.g. 50 or 75 m. Combined with a maximum velocity of 1.5 m/s the maximum time step Δt in the stability region for Δx = 50 m is 47 s and for Δx = 75 m, Δt is 70 s. The required imposed diffusion coefficient in these cases are 26.5 m^2/s and 39.5 m^2/s respectively. This means that a tidal period of 12 hours has to be simulated with approximately 920 steps for the first case and 620 steps for the second case, which is acceptable from an economical point of view. Up to now only considerations concerning stability are used to determine the numerical parameters. Based on the experience from the steady state computations with large imposed diffusion coefficients (Chapter 5), where was found that the imposed diffusion was not cancelled, the use of a smaller diffusion coefficient not exceeding some times the lateral eddy viscosity (Chapter 4) must be preferred, based upon the consideration of accuracy. The lateral eddy viscosity for a tidal channel is about 0.3 m^2/s. Computations with the use of an imposed diffusion coefficient in the order of magnitude of five times the lateral eddy viscosity will require a time step not exceeding 3 s. Of course the computation for an entire tidal period will than become excessively expensive.

A way of reducing the amount of computations without loosing stability and accuracy is the use of an implicit finite difference method in which also the convective terms are treated implicitly. Moreover the accuracy of the results may improve when the computational scheme will be set up with finite differences of a higher order. Such methods will be more expensive than the method with explicit treatment of the convective terms.

Conclusions

For the simulation of shallow-water flow an implicit finite difference method of the ADI-type is often used. Such a method can be used for flows for which the restrictions for the use of the shallow water equations hold e.g. flows in coastal water, in tidal channels and in rivers. In the computation instability can occur. One important instability originates from the explicit treatment of the convective terms in the computational scheme. The possibility of instability increases with the importance of the convective terms with respect to the other terms in the shallow-water equations. From the truncation error a stability criterion can be derived which states that an imposed diffusion coefficient dependent on the time increment size is needed in order to obtain a stable computation. A suitable time increment from an economical point of view requires a large imposed diffusion coefficient. In a steady or quasi-steaddy flow the effect of the imposed diffusion is not eliminated in the numerical computation. Therefore the imposed diffusion will influence the results of the computation severely. This influence has no relation with the influence of the physical lateral viscosity. Experiments in flumes show that the effect of the physical lateral viscosity on the flow pattern is limited to a horizontal distance near the walls of some times the depth.

For the simulation of flows in tidal channels the numerical methods have to be improved. In view of stability a modification such as an implicit treatment of the convective terms seems appropriate. Maybe a higher order scheme will improve the results.

The rectangular representation of curvilinear physical wall boundaries gives rise to numerical deviations when the grid size is large compared to the flow width. In the literature some attempts to treat the boundaries or flow parameters near the boundaries can be found in order to minimize the numerical deviation. No satisfactory treatment has been found so far.

References

Booij, N. and de Boer, S., 1981, User's guide for the program TIDES for two-dimensional tidal computations, Delft Univ. of techn., Dept. of Civil Engrg.

Booij, R. and Kalkwijk, J.P.Th., 1982, Secondary Flow in Estuaries due to the Curvature of the Main Flow and to the Rotation of the Earth and its Development, Delft Univ. of Techn., Dept. of Civil Engrg., Lab. of Fluid Mech., Internal report 9 - 82.

Fischer, H.B. et al., 1979, Mixing in inland and coastal waters, New York, Academic Press.

Flokstra, C., 1976, Generation of two-dimensional horizontal secondary currents, Delft Hydr. Lab., Research report,S163 part II.

Flokstra, C., 1981, Aspects of modelling horizontal momentum transfer in shallow flow, TOW, Report of investigations, R1150.

Kalkwijk, J.P.Th. and de Vriend, H.J., 1980, Computation of the flow in shallow river bends, Journal of Hydraulic Research 18, no. 4.

Kuipers, J. and vreugdenhil, C.B., 1973, Calculations of two-dimensional horizontal flow, Delft Hydr. Lab., Report on basic research, S163 part I

Lean, G.H. and Weare, T.J., 1979, Modelling two-dimensional Circulating flow, ASCE-proc., 105, no. HY-1.

Leendertse, J.J., 1967, Aspects of a Computational Model for Long Period Water Wave Propagation, Memorandum, RM-5294-pr, Rand Corp., Santa Monica, Calif.

Rodi, W., 1980, Turbulence Models and their application in hydraulics, IAHR.

Vreugdenhil, C.B., 1973, Secondary flow computations, 15th IAHR Congress, Istanbul.

Vreugdenhil, C.B. and Wijbenga, J.H.A., 1982, Computation of Flow Patterns in Rivers, ASCE-proc., 108, no. HY 11.

Vriend, H,J.de and Koch, F.G., 1978, Flow of water in a curved open channel with fixed uneven bed,TOW, Report on experimental and theoretical investigations, R657-VI, M 1415 part II.

Notation

C	Chézy coefficient
g	acceleration due to gravity
h	depth of flow
n	local flow coordinate perpendicular to the direction of the flow
s	local flow coordinate in the direction of the flow
T_{xx}, T_{xy}, T_{yy}	effective stresses in vertical planes
t	time
Δt	numerical time increment
u	depth averaged velocity in x-direction
u_*	bottom shear stress velocity
$\hat{u}, \hat{v}$	depth dependent values of the velocity components in x- and y-direction respectively
v	depth averaged velocity in y-direction
W_x, W_y	acceleration terms representing the surface shear stress
x	horizontal coordinate
Δx	distance between grid points
y	horizontal coordinate
z	vertical coordinate
z_b	bottom level with respect to a horizontal reference level
α	constant depending on the shape of the velocity profile
β	constant
ε_p	diffusion coefficient
ε	imposed diffusion coefficient
ζ	water level with respect to a horizontal reference level
κ	Von Karman's constant
ν	kinematic viscosity
ν_t	lateral eddy viscosity
ρ	mass density
$\overline{\rho u'^2}, \overline{\rho u'v'}, \overline{\rho v'^2}$	Reynolds stresses
$\tau_{bx}, \tau_{by}, \tau_b$	bottom shear stress
τ_w	surface shear stress
ϕ	latitude
ω	angular rotation of the earth
Ω	Coriolis parameter

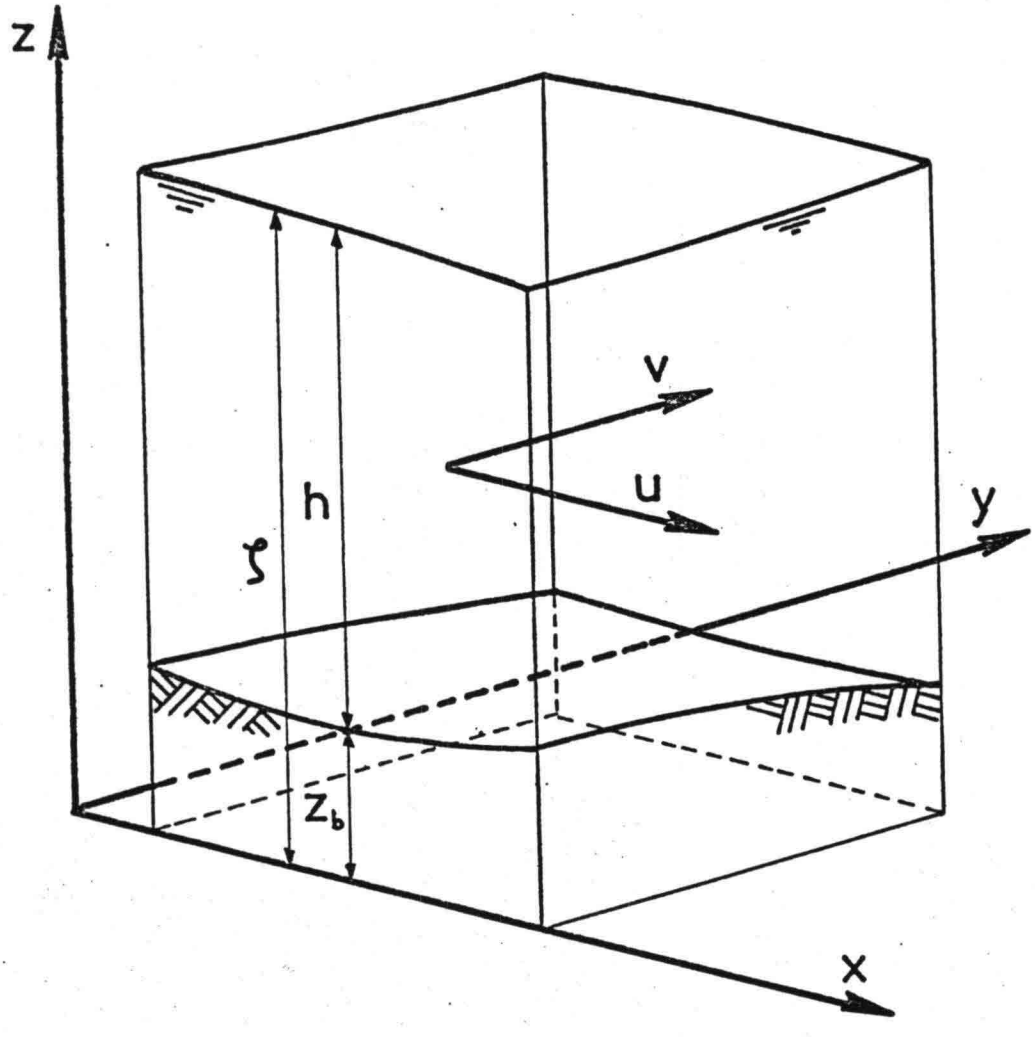

Fig. 1 Definition sketch.

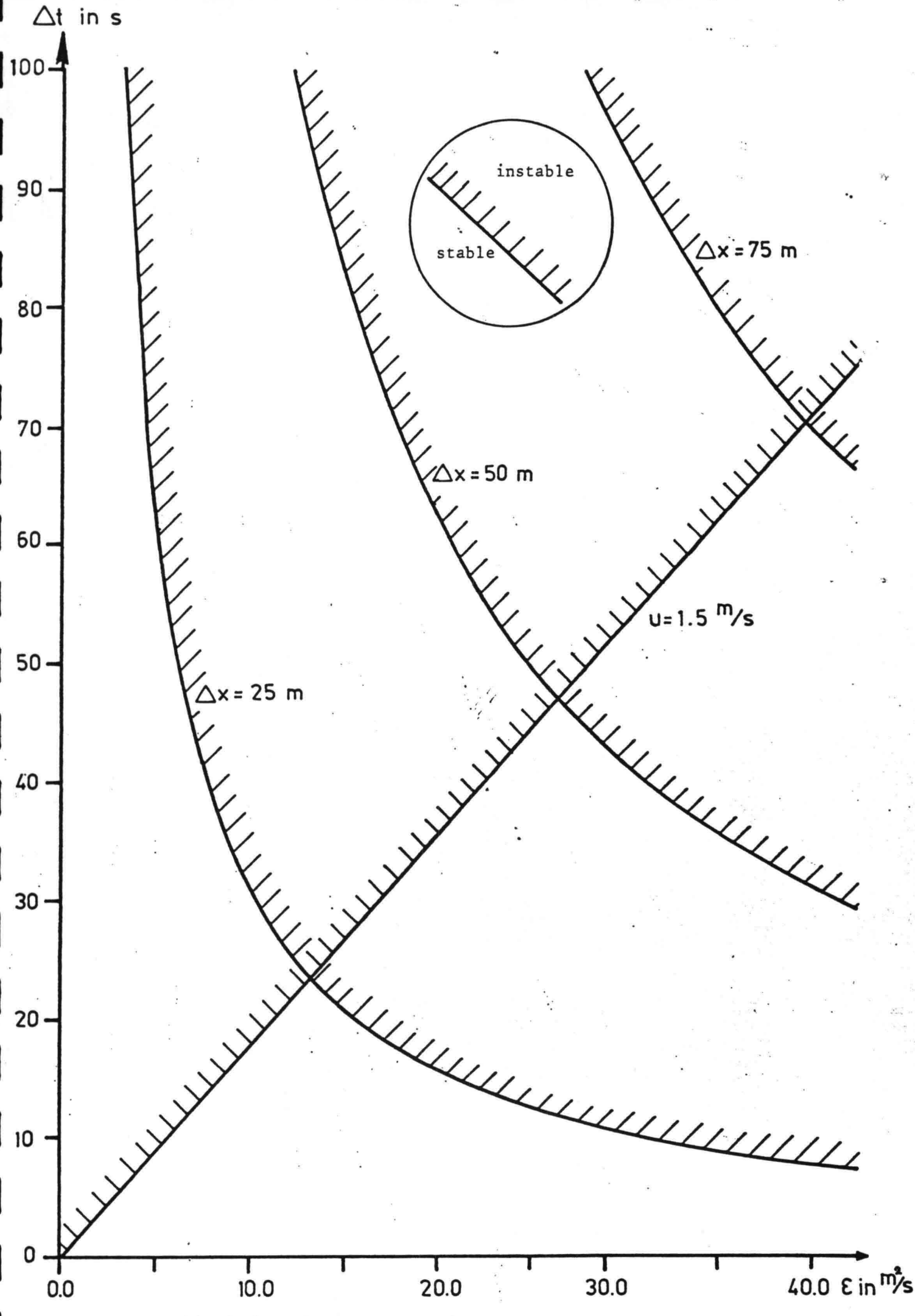

Fig. 2 Stability regions in the $\Delta t - \varepsilon$ plane.

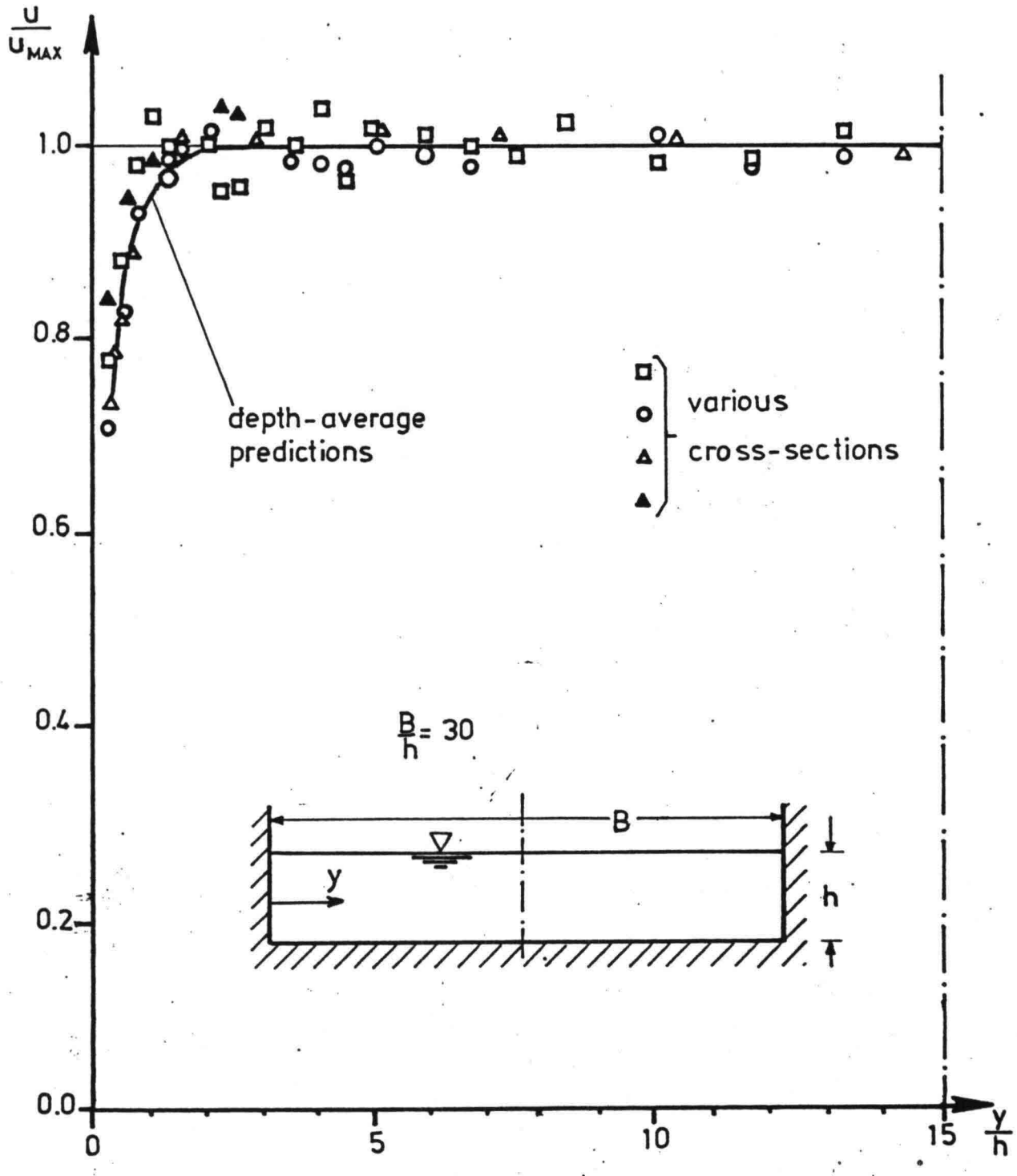

Fig. 3 Horizontal velocity distribution in developed open channel flow. (According to: Rodi, 1980)

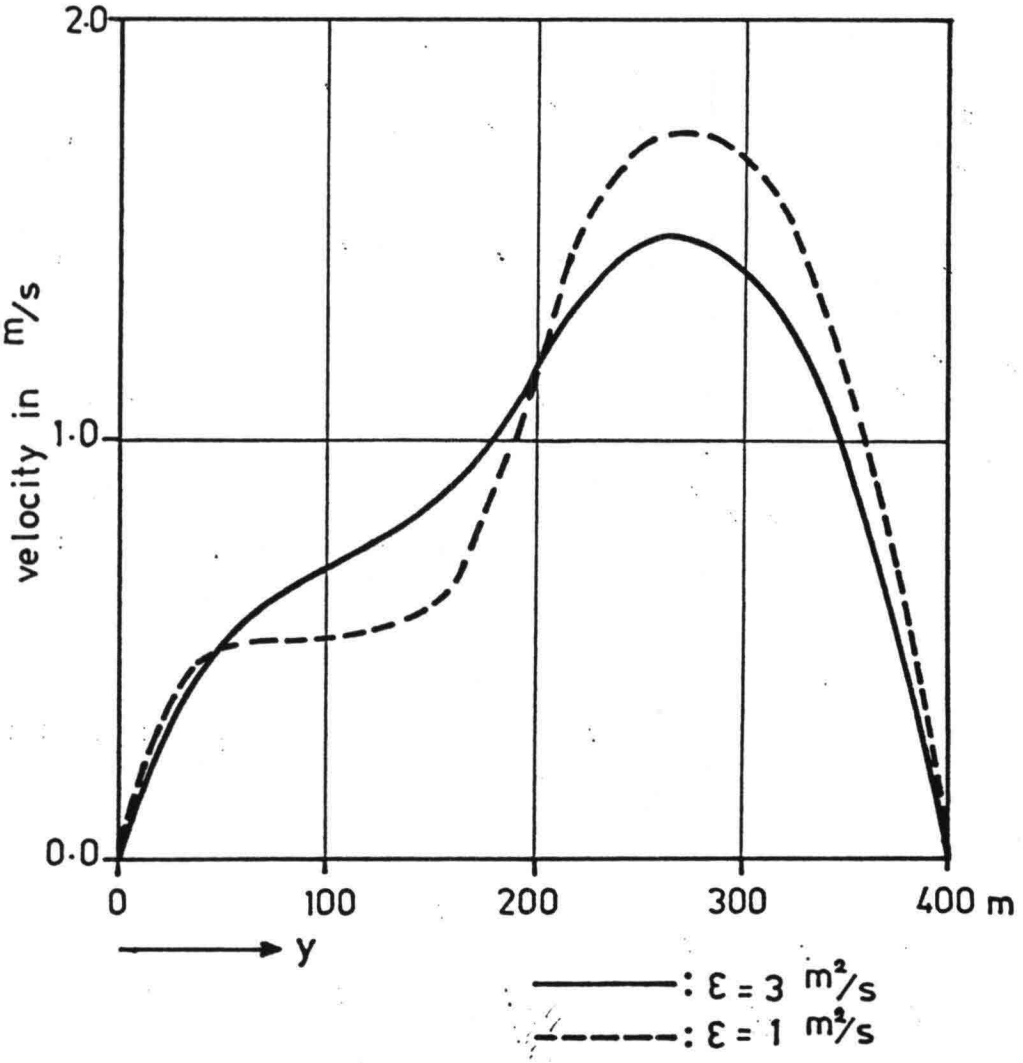

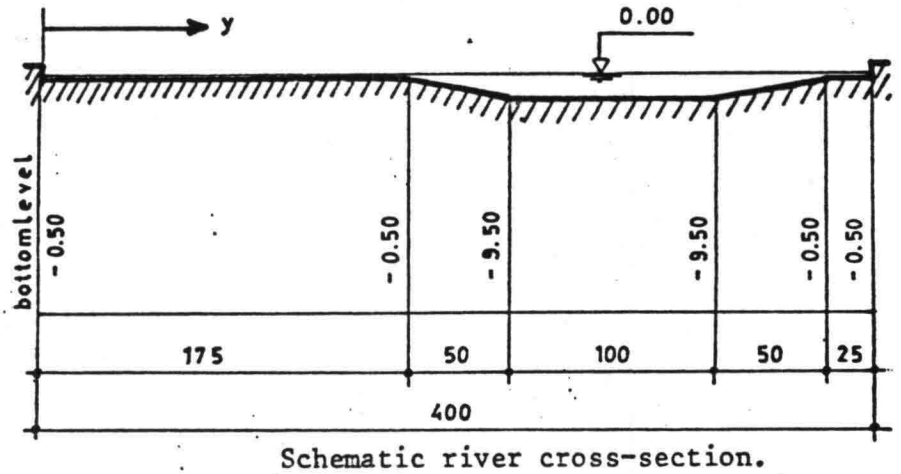

Schematic river cross-section.

Fig. 4. Computed velocity distribution for a schematic river cross-section for two different values of imposed diffusion. (According to: Vreugdenhil-Wijbenga, 1982)

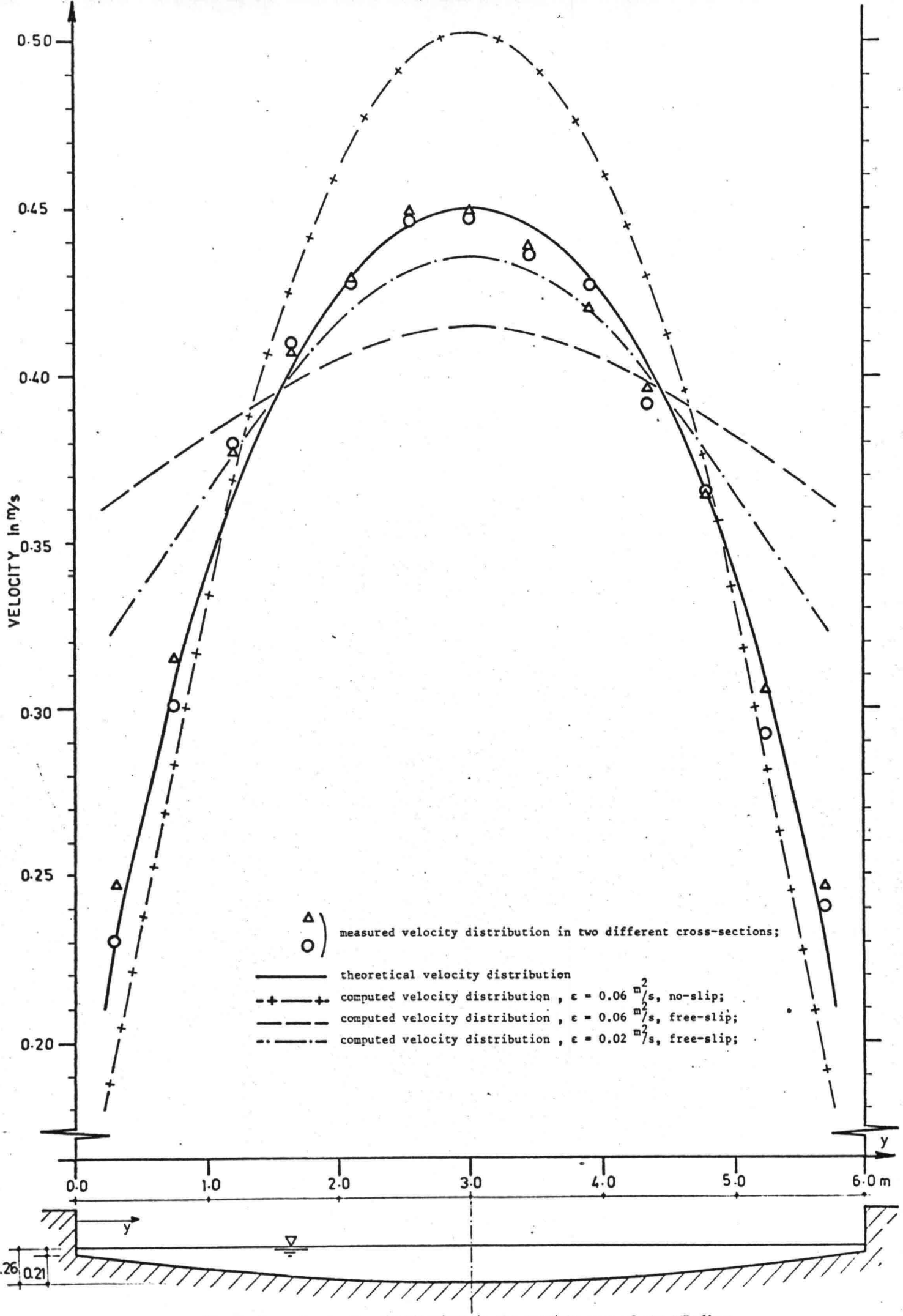

Fig. 5. Several velocity distributions in the straight part of the DHL-flume.

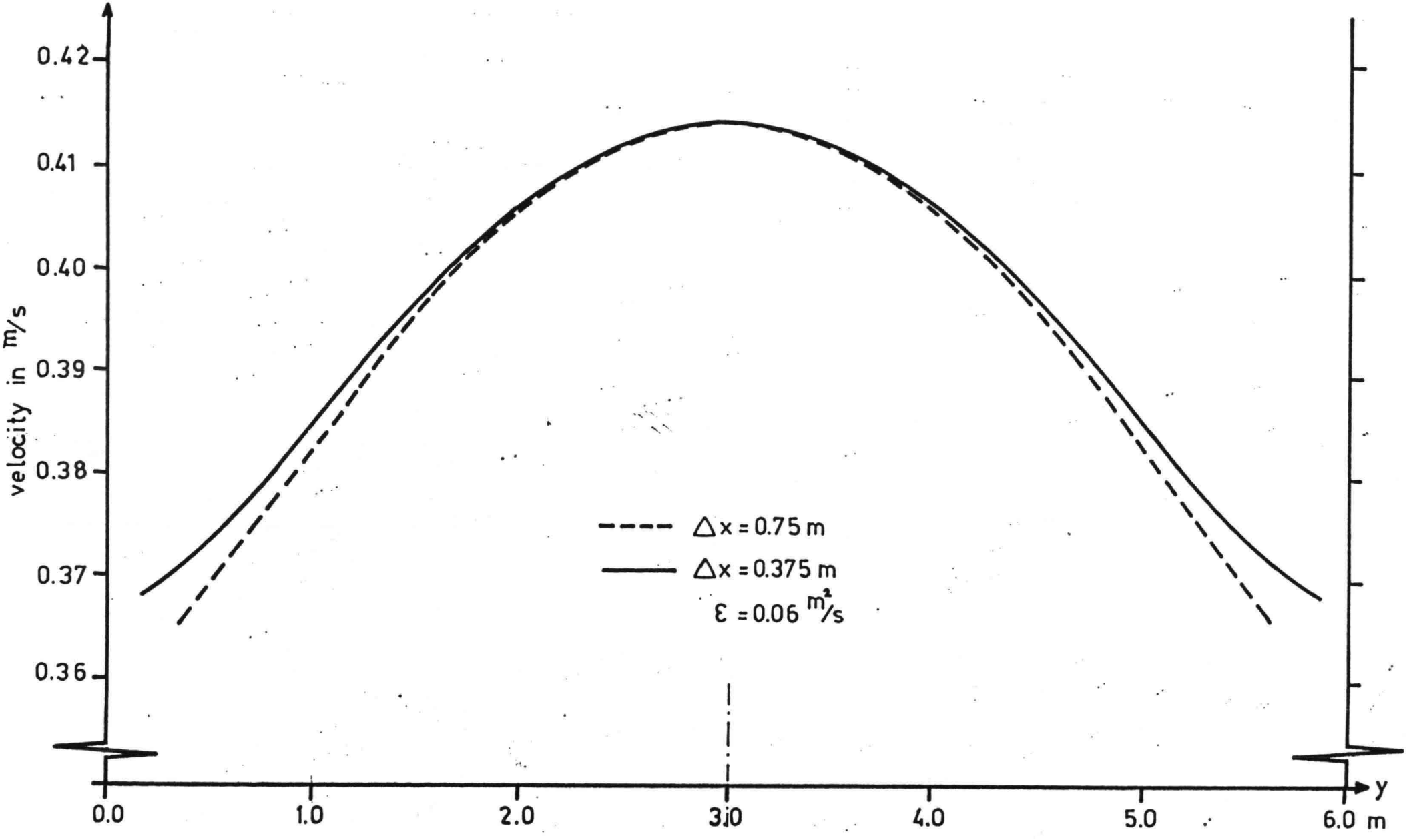

Fig. 6. Computed velocity distributions with different grid distance in the straight part of the DHL-flume.